4448 *Biochemistry* **2009,** *48,* 4448–4454
DOI:10.1021/bi802288m

BIOCHEMISTRY
including biophysical chemistry & molecular biology
Article

Probing the Kinetics and Thermodynamics of Copper(II) Binding to *Bacillus subtilis* Sco, a Protein Involved in the Assembly of the Cu_A Center of Cytochrome *c* Oxidase[†]

Thomas R. Cawthorn, Bradley E. Poulsen, David E. Davidson, Diann Andrews, and Bruce C. Hill*

Department of Biochemistry, Queen's University, Kingston, ON K71 3N6, Canada

Received December 15, 2008; Revised Manuscript Received April 14, 2009

ABSTRACT: BsSco is a member of the Sco protein family involved in the assembly of the Cu_A center within cytochrome *c* oxidase. BsSco forms a complex with Cu(II) that has properties consistent with dithiolate ligation. Stopped-flow UV−visible absorbance and fluorescence coupled with multiwavelength analysis reveal biphasic binding kinetics between BsSco and Cu(II). An initial species appears with absorbance centered at 382 nm at a copper concentration-dependent rate (2.9×10^4 M^{-1} s^{-1}). The initial species decays at a first-order rate (1.5 s^{-1}) to the equilibrium form with a maximum at 352 nm. Formation of the BsSco−Cu(II) complex is accompanied by quenching of protein fluorescence. The copper concentration-dependent phase gives 70% of the total quenching, while the final 30% develops during the second phase of the absorbance change. The pH dependence of copper binding shows that the copper-dependent rate increases by 50-fold as the pH decreases from 8.5 to 5.5 with an apparent pK_a of 6.7. The slower phase rate is independent of pH. Comparison of circular dichroism spectra between apo-BsSco and the BsSco−Cu(II) complex reveals a small change in the UV region consistent with a subtle conformational change upon copper binding. There is formation of a distinctive visible CD spectrum in the BsSco−Cu(II) complex. A model is presented in which the kinetic and thermodynamic stability of the BsSco−Cu(II) complex results from a two-step mechanism. Release of copper would be facilitated in the intermediate form of BsSco, and attaining such a low-Cu(II) affinity state may be important for BsSco's function in Cu_A assembly.

Aerobic respiratory chains employ transition metals, principally iron and copper ions, incorporated into specific protein complexes to catalyze the redox reactions from which free energy is derived to pay for the eventual formation of ATP (*1*). Cytochrome *c* oxidase is an integral membrane protein complex that terminates aerobic respiratory chains such as those found in the mitochondrial organelle and in aerobic bacteria such as *Bacillus subtilis*. Cytochrome *c* oxidase catalyzes the transfer of an electron from reduced cytochrome *c* to molecular oxygen (*2*). Members of the cytochrome *c* oxidase family of enzymes are equipped with four redox active metal centers, two heme-based centers and two copper-based centers. The heme centers both incorporate heme A in unique protein environments within the largest subunit (i.e., subunit I) and are known as cytochrome *a* and cytochrome a_3. The iron ion of the cytochrome a_3 heme is located ~5.5 Å from Cu_B, and together, these two metals form the site of O_2 binding, activation, and reduction (*3*).

The second copper center is known as Cu_A and is composed of two copper ions assembled in a highly cooperative structure that is housed within subunit II of the oxidase complex. The two copper ions of the Cu_A center are located within bonding distance of one another and are bridged by two cysteine sulfur side chains. The dinuclear Cu_A center is poised in an unusual mixed-valence state such that in its oxidized form each of the two copper ions has a formal valence state of +1.5 (*4*). The Cu_A center serves as the initial electron acceptor from reduced cytochrome *c* and upon reduction is diamagnetic with each ion in the +1 state. Cu_A returns to its oxidized state by passing one electron on to cytochrome *a*, which in turn passes one electron at a time to the cytochrome a_3-Cu_B center (*5*). Cytochrome *a* and Cu_A thus serve as intermediaries in the passage of reducing equivalents from cytochrome *c* to the oxygen binding site.

The Sco family of proteins is known to play a role in assembly of the Cu_A center of cytochrome *c* oxidases. The Sco proteins have a thioredoxin core structure and loops that are extraneous to the thioredoxin core (*6*−*8*). One of these loops contains a pair of conserved cysteine residues in a CXXXC sequence, and a second loop located ~100 amino acids from the cysteine pair in the primary sequence contains a conserved histidine. These three residues are conserved in the structure of the Sco proteins from *B. subtilis* (i.e., BsSco),[1] yeast, and humans and are known to be critical to Sco's role in Cu_A assembly (*9*, *10*). Several specific roles

[†]This work was supported by a Discovery Grant and an Equipment Grant to B.C.H. from the Natural Science and Engineering Research Council (Canada) and an Infrastructure Grant from the Canadian Foundation for Innovation to the Protein Function Discovery group at Queen's University.

*To whom correspondence should be addressed. Phone: (613) 533-6375. Fax: (613) 533-2497. E-mail: hillb@queensu.ca.

[1]Abbreviations: BsSco, Sco1 homologue from *B. subtilis*; CD, circular dichroism.

Published on Web 4/15/2009

have been proposed for Sco in the assembly of the Cu_A center. For example, Sco's relationship to thioredoxin has led to the suggestion that Sco could act as a disulfide exchange protein to reduce the two cysteine residues of the Cu_A center (*7*, *11*). Evidence of a disulfide exchange function for the Sco homologue in *Thermus thermophilus* has recently been presented (*12*). Alternatively, Sco's copper binding properties have led to the proposal that Sco acts as a metal chaperone to deliver copper to the Cu_A site (*13*). The presence of proteins with a high degree of sequence similarity to Sco in bacterial species that do not make Cu_A like centers has led to the proposal of a role for Sco in response to the generation of reactive oxygen species (*14*). Regardless of the exact nature of Sco's function in various biological systems, its interaction with copper may have an important role to play as an intermediate in copper delivery or in stabilizing the reduced form of Sco for eventual disulfide exchange.

We have shown in equilibrium binding experiments that BsSco prefers Cu(II) to Cu(I) by more than 1 million-fold (*15*). This is in contrast to mitochondrial Sco1 that has been characterized as a Cu(I) binding protein (*10*). The difference in copper redox state preference is proposed to reflect the different environments of the *B. subtilis* and mitochondrial versions of Sco. Mitochondrial Sco1 is located within the inner mitochondrial membrane in a reducing environment that provides Cu(I) and only small amounts of Cu(II) (*16*), whereas BsSco is located on the outer surface of the *B. subtilis* plasma membrane and exposed to an oxidizing environment. We have measured the rate of interaction of reduced BsSco with copper(II) ions by time-resolved fluorescence and absorption. The reaction is found to occur as a two-step process with an initial copper complex delineated by an absorption maximum at 382 nm that is red-shifted compared to the final copper complex of BsSco that absorbs at 352 nm. The pH dependence of the binding reaction shows that the first step increases in rate as the pH is lowered, whereas the second rate is independent of pH. The kinetics combined with the equilibrium constant for copper binding indicates that the initial complex is relatively weak and the second step contributes substantially to the overall binding affinity. The two-step binding mechanism has implications for the mechanism of release of copper by BsSco. If the mechanism occurs by a reversal of the binding reaction, there has to be a mechanism for promoting the dissociation of the kinetically inert BsSco−Cu(II) complex.

MATERIALS AND METHODS

Wild-type and mutant versions of recombinant BsSco were expressed as fusion proteins with glutathione *S*-transferase in *Escherichia coli* and purified by affinity chromatography (*17*). The fusion proteins were cleaved using thrombin, and thrombin was removed when the samples were passed over benzamidine-linked Sepharose. The purity of the BsSco preparations were assessed by denaturing polyacylamide electrophoresis as described previously (*18*).

The concentration of BsSco was determined by absorption spectrophotometry using an extinction coefficient at 280 nm of 19.2 mM^{-1} cm^{-1}. The redox state of BsSco was determined by reaction with the sulfhydryl reactive reagent 4,4′-dipyridyl disulfide using an extinction coefficient of 18.8 mM^{-1} cm^{-1} for the thiopyridone product (*19*). The amount of copper binding to BsSco was determined by the extent of formation of the absorbance band at 352 nm with an extinction coefficient of 4.78 mM^{-1} cm^{-1} (*20*).

Rapid-scanning stopped-flow kinetics was performed on an OLIS RSM1000 spectrometer fitted with an OLIS USA stopped-flow apparatus. In absorbance mode, the scanning monochromator was fit with a 0.2 mm slit giving a 2 nm bandpass. In the fluorescence mode, excitation was at 280 nm with a bandpass of 4 nm for both the excitation and emission monochromators. Analysis of multiwavelength data sets was conducted using the Specfit software package (Spectrum Software Associates).

UV and visible CD spectra were recorded on a Chirascan instrument from Applied Photophysics. Spectra were collected from 260 to 180 nm at an interval of 1 nm, with an integration time of 0.5 s and a cell path length of 0.1 mm. In the visible region, spectra were recorded from 600 to 250 nm at an interval of 1 nm, with an integration time of 0.5 s and a path length of 2 mm. In both spectral regions, the bandpass used was 1 nm.

RESULTS

We have characterized the equilibrium binding constant of BsSco for Cu(II) and Cu(I) to show that BsSco prefers Cu(II) (K_D = 3.5 pM) by more than 1 million-fold over Cu(I) (K_D = 10 μM) (*15*). The equilibrium BsSco−Cu(II) species is stable kinetically and shows no dissociation after 5 days at room temperature (*15*). Moreover, we observe that the UV CD spectrum of the BsSco−Cu(II) complex is unchanged over 5 days and so conclude that the overall structural integrity of the protein is stable over this period. In this work, we examine the kinetics of copper binding to BsSco by rapid-scanning stopped-flow absorption and fluorescence. Figure 1 illustrates the reaction of reduced BsSco at pH 7.0 with copper(II). Panel A shows a set of spectra collected every 200 ms for 3 s over the wavelength range from 300 to 450 nm. The reaction leads at long times to the formation of a species with an absorption maximum at 352 nm that is identical to that reported previously from equilibrium binding experiments (*20*). However, the growth of an intermediate with a spectral contribution at longer wavelengths is also observed at earlier times. This can be seen clearly by looking at selected wavelengths over time (Figure 1B). At 400 nm (B, trace ii), there are growth and decay phases evident, whereas at 350 nm, a simple increase is apparent (panel B, trace i). The three-dimensional data set of absorbance versus wavelength versus time is subjected to multiwavelength analysis that begins with singular-value decomposition to yield estimates of the number and form of the spectral and kinetic components of the matrix describing this system (*21*). The data are then fit to a three-component sequential model in which the initial metal-free form of BsSco forms an intermediate that decays to the final copper complex. The smooth lines through the absorbance time courses are the results of this kinetic fit. Trace iii (Figure 1B) shows an example of the distribution of residuals between the model and the data at 400 nm.

This approach also yields estimates of the three spectral species proposed for the model (Figure 2A,B) and their population over time (Figure 2C). Panel A shows absolute spectra for the initial apo-BsSco species, the intermediate, and final copper-bound BsSco, whereas panel B shows difference spectra of the copper-bound forms of BsSco with the spectrum of the apo species used as a reference. The initial intermediate has a spectral maximum at 382 nm with an extinction coefficient smaller than that of the final copper-bound form. The time courses for the three forms of BsSco show that the apo species disappears over the first second, the intermediate state reaches a maximum level of 55% of the

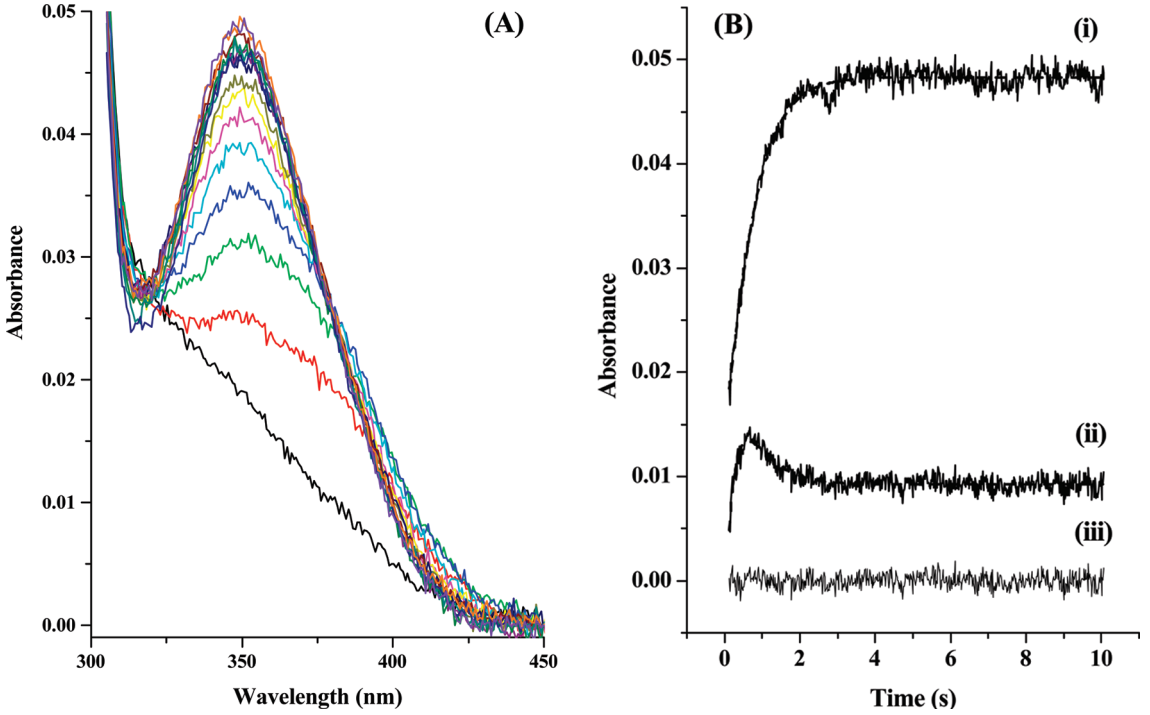

FIGURE 1: Copper(II) binding to BsSco. Reduced apo-BsSco was mixed with $CuCl_2$ in a stopped-flow apparatus, and absorption spectra were recorded via rapid-scanning spectrophotometry over the wavelength range from 300 to 450 nm. The final concentration of BsSco is 25 μM, and that of $CuCl_2$ is 112.5 μM in 25 mM sodium phosphate (pH 7.0). The experiment was performed at 20 °C. The path length of the stopped-flow cuvette was 4 mm. Spectra were collected at a rate of 63 scans per second. (A) Fifteen spectra are displayed that were collected at intervals of 208 ms over a total time of 3.12 s. The spectrum with the lowest absorbance at 350 nm is just after mixing and corresponds to time zero. (B) The kinetics of copper binding are illustrated at two wavelengths, (i) 350 and (ii) 400 nm. The smooth line through the data is the result of the global analysis of the entire data set to a two-step binding model. Trace iii shows an example of the distribution of residuals at 400 nm between the data and the model.

total BsSco population at 0.42 s, and the final species becomes the sole form at times longer than 3 s.

When the stopped-flow absorption experiment is repeated as a function of the copper concentration, we observe that the rate of the first step increases in proportion to the copper concentration whereas the rate of the second step is unchanged. Therefore, we propose that the mechanism of copper binding to BsSco is a two-step process (see 1 below) with the first step being a bimolecular reaction with a rate of $(2.99 \pm 0.41) \times 10^4$ M^{-1} s^{-1} and a second step that is unimolecular with a first-order rate of 1.5 ± 0.16 s^{-1}.

$$\text{BsSco} + \text{Cu(II)} \xrightarrow[k_1 = 3\times10^4 M^{-1}s^{-1}]{} \overset{\lambda_{max}=382nm}{\text{BsSco•Cu(II)}*} \xrightarrow[k_2 = 1.5s^{-1}]{} \overset{\lambda_{max}=352nm}{\text{BsSco}-\text{Cu(II)}} \quad (1)$$

BsSco exhibits intrinsic protein fluorescence arising primarily from two tryptophan residues within its primary structure. In the native folded state of BsSco, the two tryptophans are located approximately 15 Å (i.e., W101) and 24 Å (i.e., W36) from the copper-binding site. The intrinsic fluorescence intensity of BsSco is critically dependent on the state of the metal binding site (*15*). The most highly fluorescent form is reduced, apo-BsSco, whereas the fluorescence is heavily quenched when the two thiol residues are in the oxidized cystine form (*22*) or are bound to Cu(II). The mechanism of metal quenching of tryptophan fluorescence is complex (*23*), but in the case of the BsSco−Cu(II) complex, there is some degree of energy transfer that is dependent on spectral overlap of the donor and acceptor species and the distance between these two sites. We used stopped-flow mixing to measure the transient change in intrinsic fluorescence that occurs as BsSco binds Cu(II). Figure 3A shows time-resolved emission spectra taken after rapid mixing of reduced apo-BsSco with excess $Cu(II)Cl_2$. The emission intensity is observed to decrease by 50% over the 2 s time course, while the emission maximum remains at 330 nm over the entire course of the binding reaction. When the three-dimensional data set is subjected to global analysis, two kinetic phases are resolved (e.g., Figure 3B) with observed rate of 16.5 and 1.6 s^{-1}. These two phases follow the same pattern with respect to copper concentration dependence that were observed for the transient absorbance data. Thus, the fast phase rate is copper concentration-dependent with a bimolecular rate constant of 3.2×10^4 M^{-1} s^{-1}, whereas the second phase is independent of copper concentration with a first order rate of 1.6 s^{-1}. The spectral components are also derived from this analysis and are shown in Figure 3C. The emission spectrum of the starting material gives the strongest signal, and following the fast phase of fluorescence decline, the intermediate has a lower emission intensity, which then decays to the final form with the lowest intensity. The overall decline in emission intensity observed here is ~50%; 70% of that change occurs in the initial fast phase of the reaction, while the final 30% of the intensity change develops at the slower rate. The constant emission maximum indicates that there are no changes in the environment of the tryptophan residues that are linked to copper binding. Thus, the initial intermediate in BsSco's reaction with Cu(II) has an absorption spectrum centered at 382 nm, and the majority of the quenching is established. As the 382 nm intermediate evolves to the 352 nm form, the increase in quenching intensity probably arises from a better spectral overlap of the donor tryptophans and the acceptor (i.e., copper center). The position of the copper

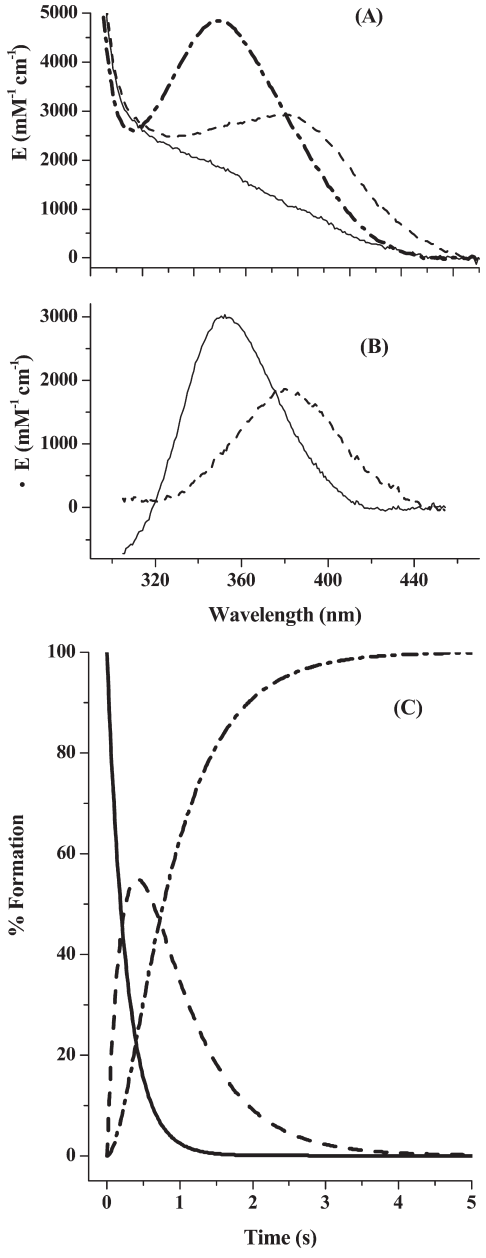

FIGURE 2: Forms and lifetimes of BsSco observed during copper binding. Spectral intensity is plotted on a scale of extinction coefficient based on a path length of 1 cm. (A) Time-resolved spectra generated by multiwavelength analysis of the reaction of BsSco with copper. Absolute spectra are shown for the apo-BsSco (—), initial intermediate (—), and final copper-bound forms of BsSco (—·—). (B) Difference spectra are shown for the final (—) and intermediate (—) copper-bound forms of BsSco with the spectrum of apo-BsSco as a reference. (C) Populations of the apo-BsSco (—), intermediate (—), and final (—·—) copper-bound BsSco as a percentage of the total are plotted vs time.

in its binding site relative to the tryptophan residues would be largely unchanged as the 382 nm intermediate of BsSco changes to the final copper-bound form. Thus, the initial copper complex of BsSco has the metal well integrated into the protein matrix.

Formation of the equilibrium BsSco−Cu(II) complex involves ligation of the copper by three conserved amino acids, two cysteines (C45 and C49) and one histidine (H135), and probably one water taking a fourth ligand position (*11*, *20*). We presume that it is the deprotonated forms of these side chains that are acting as inner sphere metal ligands, and thus, their respective microscopic pK_a values could be an important determinant in the mechanism of copper binding. We measured, therefore, the copper binding kinetics as a function of pH by stopped-flow, transient absorption spectroscopy. A sample of the multiwavelength data set collected at pH 5.5 shows evidence again of two spectral components in the reaction (Figure 4A). Time courses at individual wavelengths show distinct phases of growth and decay at 400 nm and an initial lag phase at 350 nm followed by a continual absorbance increase over 1.5 s. In addition, the shapes of these time courses support the sequential nature of the kinetic model. The smooth lines through these time courses are the fits to the data from a model with two rate constants defining the kinetic conversion of three species of BsSco (Figure 4B). The time courses of the BsSco species show a disappearance of apo-BsSco much faster than that observed at pH 7.0 and a sharper rise in the intermediate, which reaches a level of more than 80% at 0.2 s (Figure 4C). The spectral forms of BsSco are the same as those derived from the multiwavelength fitting obtained at pH 7.0. In addition, we observe that the UV CD spectrum of apo-BsSco is not discernibly different over the pH range from 5.5 to 8.5. Thus, the nature of the intermediates of BsSco does not change over the pH range explored, but their disposition in time is altered.

A plot of the observed rates at a copper concentration of 200 μM for the two phases versus pH is shown in Figure 5. The first step increases in rate by ~50-fold going from pH 8.5 to 5.5. The second-order rate constant for formation of the intermediate form of BsSco is 9.5×10^4 M^{-1} s^{-1} at pH 5.5. In contrast, the rate of the second phase is constant, at ~1.5 s^{-1}, across the pH range studied here. There is an inflection point for the pH dependency of the fast phase at a pH of 6.70. As the pH is lowered, the rate of formation of the initial copper complex of BsSco increases, and we conclude, therefore, that deprotonation of the ligating amino acid side chains is not a rate-determining step for the initial copper binding.

Formation of the final complex of BsSco with Cu(II) may be limited by a protein conformational change. We assessed the occurrence of a protein conformation change by measuring the CD spectra over the UV range in the absence and presence of copper (Figure 6A). In addition, we recorded the CD spectrum of the equilibrium complex across the visible region (Figure 6B). The UV CD spectrum of apo-BsSco is entirely consistent with the spectrum reported previously and the crystal structure showing a protein with both α-helical (26%) and β-sheet (22%) secondary structural components (*7*). We know from the crystal structure that ligation of Cu(II) by two cysteine residues and one histidine requires a conformational change because the histidine side chain is more than 10 Å from the cysteine pair. Addition of 1 equiv of Cu(II) to this sample gives full formation of the BsSco−Cu(II) complex, consistent with the high affinity of BsSco for copper(II). There is very small change in the UV CD signal that accompanies copper(II) binding. Binding of copper does give rise to a distinct visible CD spectrum with maxima at 344 and 459 nm and minima at 385 and 586 nm. Forms of BsSco that do not bind copper such as the oxidized, wild-type protein or a mutant in which one of the three ligating residues is altered (e.g., C45S or C49S) do not show a change in the UV CD upon copper addition and do not have a visible CD spectrum. These data taken together with the lack of a UV CD change of apo-BsSco across the measured pH range imply that copper binding drives the conformational change in BsSco.

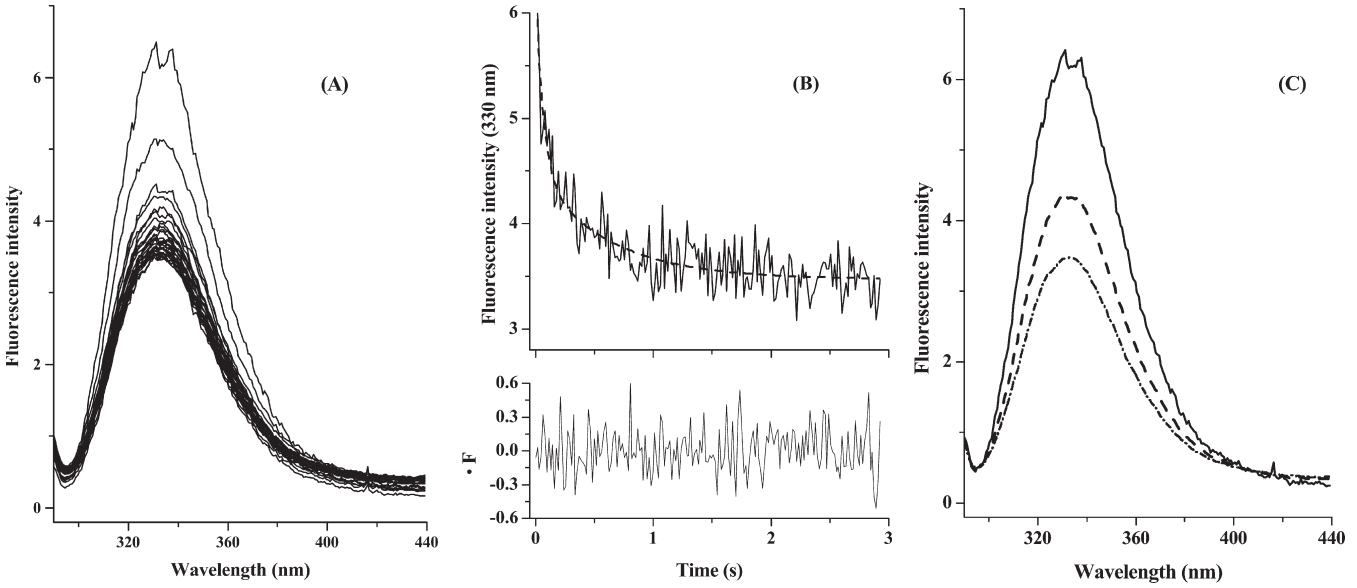

FIGURE 3: Time-resolved fluorescence quenching during the reaction of BsSco with copper. Reduced apo-BsSco was mixed with copper in a stopped-flow apparatus, and emission spectra were recorded at a rate of 63 per second. The fluorescence excitation was at 280 nm, and the bandpasses for excitation and emission were both set at 4 nm. The final concentration of BsSco is 20 μM, and that of $CuCl_2$ is 500 μM in 25 mM sodium phosphate (pH 7.0) at 20 °C. (A) Forty-five emission spectra are displayed at 63 ms intervals over 2.89 s of the reaction. The initial spectrum obtained just after mixing gives the largest signal, and the intensity declines over time. (B) Time course of fluorescence quenching at 330 nm. Trace i is the data set, and the smooth line is the fit from the two-step model. The residual difference at 330 nm between the model and the data is shown in trace ii. (C) Time-resolved emission spectra from multiwavelength analysis for (—) apo-BsSco, (—) the initial copper−BsSco intermediate, and (—·—) the final copper−BsSco complex.

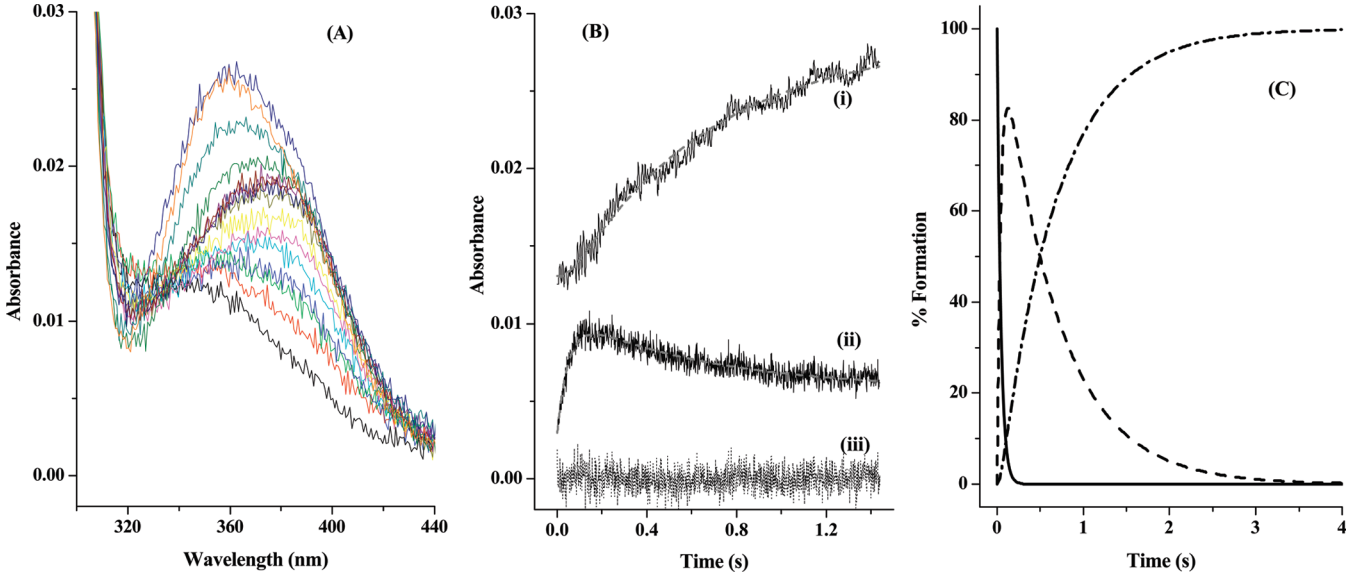

FIGURE 4: Time-resolved absorption spectra for the reaction of BsSco with copper at pH 5.5. Spectra were recorded at 1 ms intervals for 1.5 s following the mixing of BsSco with copper. The final concentration of BsSco is 15 μM, and that of $CuCl_2$ is 100 μM in 25 mM sodium phosphate (pH 5.5) at 20 °C. (A) The spectrum at time zero gives the lowest intensity at 380 nm. The first 10 spectra of increasing intensity are displayed at 10 ms intervals and the final five spectra at 100 ms intervals. (B) The kinetics of the absorbance change is illustrated by time courses at (i) 352 and (ii) 400 nm. The smooth line through the data is the two-component fit. Trace iii is an illustration of the residuals between the model and the data at 400 nm. (C) Population of the intermediate state of BsSco over time at pH 5.5. The forms of BsSco are indicated as (—) apo-BsSco, (—) the initial copper−BsSco intermediate, and (—·—) the final copper−BsSco complex.

DISCUSSION

Scheme 1 shows a model for the interaction of Cu(II) with BsSco. We have shown in previous work that BsSco has a very high affinity for Cu(II) (K_D = 3.5 pM) (*15*). The findings reported here reveal that this high affinity is the result of a two-step binding mechanism. The first step in copper binding is a bimolecular process that produces an intermediate that undergoes an isomerization step to yield the final form. Previous measurements of the kinetic stability of the equilibrium copper complex of BsSco show that the dissociation of the complex is exceedingly slow. The BsSco−Cu(II) species (*15*) and the overall protein structure (vide supra) are stable on the order of days at room temperature in the absence of any excess copper ($t_{1/2}$ > 5 days). Because there is no accumulation of the BsSco·Cu(II)* intermediate during dissociation, we assign the slow dissociation rate to the k_{-2} step. This allows us to estimate the equilibrium

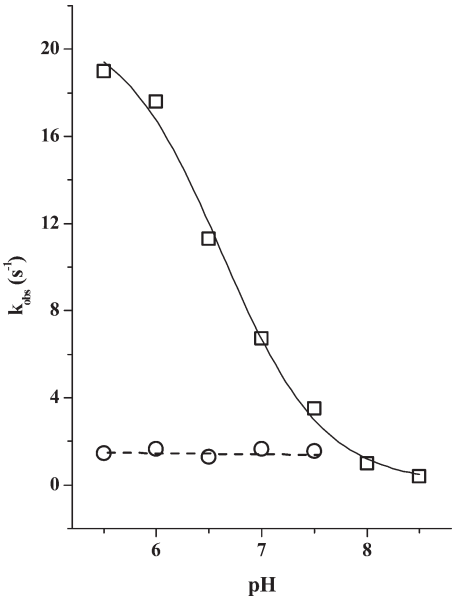

FIGURE 5: Kinetics of copper binding to BsSco as a function of pH. Observed rates for copper binding were estimated from stopped-flow-derived multiwavelength time courses that were fit to a two-step model. The final concentration of BsSco is 25 μM, and that of $CuCl_2$ is 200 μM in 25 mM sodium phosphate at the indicated pH. The fast phase rate (□) and the slow phase rate (○) are plotted vs pH. The line through the fast phase data is from a single protonation site model with a pK_a of 6.70.

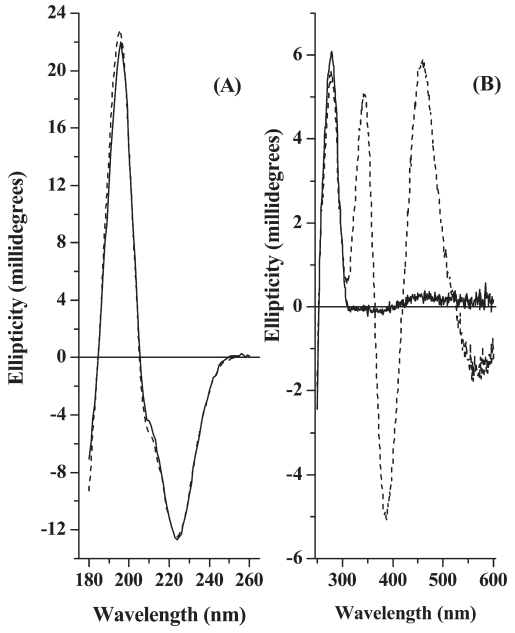

FIGURE 6: Circular dichroism spectra of apo-BsSco and the BsSco−Cu(II) complex in the UV and visible regions. The concentration of BsSco is 1.83 mg/mL in 10 mM sodium phosphate (pH 7.0). The BsSco−Cu(II) sample contains 95 μM $CuCl_2$, or approximately 1 equiv of copper per BsSco. The solid line spectra are for the apoprotein, and the dashed line spectra are for the copper complex of BsSco. Other conditions are given in Materials and Methods.

binding contribution of each step to the overall binding constant and the dissociation rate constant k_{-1}. These values are shown in Scheme 1. The second step provides almost 10^6 in additional equilibrium stability. The bottom part of scheme depicts the equilibrium energetic relationship of the three BsSco forms and the kinetic barriers to their interconversion. In this scheme, the largest constraint in a kinetic sense for the release of copper and

Scheme 1: Two-Step Binding of Cu(II) to BsSco and Energetic Relationships between the Forms of BsSco

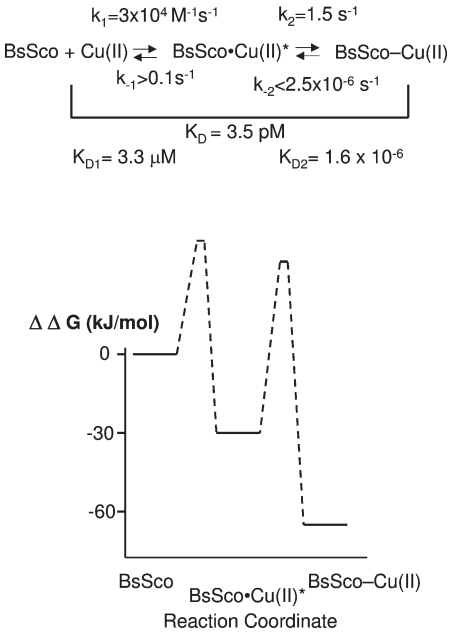

free BsSco is the microscopic dissociation rate constant, k_{-2}, for generating the intermediate form of the BsSco·Cu complex.

The extreme kinetic stability of the BsSco−Cu(II) complex presents a potential problem if BsSco functions in copper transfer (*24*) or in disulfide exchange to apo-Cu_A (*12*). Our binding model suggests how the kinetic inertness of the BsSco−Cu(II) complex can be overcome. In the two-step binding mechanism, the kinetic stability derives from the slow microscopic rate of conversion of the BsSco−Cu(II) complex to the intermediate form. If the intermediate form of the complex can be stabilized, then the process of copper release is facilitated. For example, an interaction involving acidic residues in the histidine loop of BsSco with basic residues within subunit II could facilitate copper release. This would allow BsSco to function in copper transfer to apo-Cu_A or release reduced apo-BsSco for participation in disulfide exchange to generate reduced apo-Cu_A. A conformation of BsSco with a low affinity for copper is implied in our structural studies in which we could not find conditions to stabilize the copper complex of BsSco in the crystal form (*7*). The structure of BsSco that we observed in the crystal may be the conformation of BsSco with a low affinity for copper. However, alternative mechanisms for release of copper from BsSco such as a redox-triggered process in which BsSco is oxidized and Cu(I) is released must also be considered. Such a mechanism would effectively bypass the kinetic stability of the BsScoCu(II) species observed here.

The increase in the binding rate of BsSco as the pH is lowered is somewhat unanticipated because each of the protein ligands binds in the unprotonated state. This implies that deprotonation of any of these three residues is not rate-limiting with respect to the formation of the initial copper complex. However, protonation at some site on the protein is rate-determining as evidenced by the 50-fold increase in rate as the pH is lowered. The pK_a of 6.70 suggests histidine as a likely residue. Since only the ligating histidine is conserved in BsSco, it is feasible that the protonation of this residue breaks an interaction within the apo-BsSco structure that gives the histidine loop the freedom to move into a copper binding position. This initial complex then relaxes in an

intramolecular first-order process to the final tightly bound BsSco−Cu(II) complex. However, the structure of BsSco shows that the position of the conserved histidine is solvent-exposed and no hydrogen bonds between it and the rest of the protein are observed (*25*). It is possible that an interaction within the protein at a site remote from the metal binding ligands might play a role in allowing the binding site to form. For example, there is an interaction between asparagine 44, situated in the cysteine loop, and aspartate 78 that could mediate the pH sensitivity of copper binding. The initial BsSco·Cu(II) complex has an absorption maximum at 382 nm that we propose arises from a ligand to metal charge transfer complex that would be consistent with binding of at least one of the conserved cysteine residues that are known to be inner sphere ligands in the final Cu(II)−BsSco complex. The shift to a lower energy of the charge transfer band in the intermediate is consistent with a lower covalency of this interaction. However, any specific assignment of the ligand field in the intermediate is premature at this point. The molecular mechanism involved in this process will require more detailed investigation. For example, we have initiated a rapid freeze quench EPR study to better characterize the ligation state of the transient intermediate in the reaction of BsSco with Cu(II). Although further work is required to make our assignment definitive, we can say at this stage that the time-resolved EPR spectrum of the initial intermediate is different from that of the equilibrium species, indicating that rearrangement of the ligand field has occurred over the binding process (Bennett and Hill, unpublished observation).

Transfer of copper into a construct of apo-Cu_A from a soluble construct of the copper binding protein PCu_AC has been demonstrated in vitro for the proteins derived from *T. thermophilus* (*12*). In this system, the current view is that the *T. thermophilus* version of Sco serves the role of a disulfide exchange protein specific for apo-Cu_A to maintain the two cysteines in this protein in the reduced state and available for copper ligation. In the mitochondrial system, however, evidence of the transfer of copper from Cox17 to Sco1 has been presented (*26*). A homologue of the PCu_AC protein has not been found in *B. subtilis*, or in mitochondria, and therefore, a role for BsSco in the transfer of copper to apoCu_A in *B. subtilis* cannot be ruled out. Perhaps the Sco family of proteins has adapted to play a distinct role in the circumstances present in each of these biological situations. Further work on the copper transfer mechanism in the *B. subtilis* system will be pursued in this light.

ACKNOWLEDGMENT

We are grateful to Mr. Kim Munro of the Protein Function Discovery Group for assistance with the OLIS rapid-scanning spectrometer.

REFERENCES

1. Genova, M. L., Baracca, A., Biondi, A., Casalena, G., Faccioli, M., Falasca, A. I., Formiggini, G., Sgarbi, G., Solaini, G., and Lenaz, G. (2008) Is supercomplex organization of the respiratory chain required for optimal electron transfer activity?. *Biochim. Biophys. Acta 1777*, 740–746.
2. Hosler, J. P., Ferguson-Miller, S., and Mills, D. A. (2006) Energy Transduction: Proton Transfer Through the Respiratory Complexes. *Annu. Rev. Biochem. 75*, 165–187.
3. Brzezinski, P., Reimann, J., and Adelroth, P. (2008) Molecular architecture of the proton diode of cytochrome c oxidase. *Biochem. Soc. Trans. 36*, 1169–1174.
4. Solomon, E. I., Xie, X., and Dey, A. (2008) Mixed valent sites in biological electron transfer. *Chem. Soc. Rev. 37*, 623–638.
5. Hill, B. C. (1994) Modeling the sequence of electron transfer reactions in the single turnover of reduced, mammalian cytochrome *c* oxidase with oxygen. *J. Biol. Chem. 269*, 2419–2425.
6. Balatri, E., Banci, L., Bertini, I., Cantini, F., and Ciofi-Baffoni, S. (2003) Solution structure of Sco1: A thioredoxin-like protein involved in cytochrome *c* oxidase assembly. *Structure 11*, 1431–1443.
7. Ye, Q., Imriskova-Sosova, I., Hill, B. C., and Jia, Z. (2005) Identification of a disulfide switch in BsSco, a member of the Sco family of cytochrome *c* oxidase assembly proteins. *Biochemistry 44*, 2934–2942.
8. Abajian, C., and Rosenzweig, A. C. (2006) Crystal structure of yeast Sco1. *J. Biol. Inorg. Chem. 11*, 459–466.
9. Mattatall, N. R., Jazairi, J., and Hill, B. C. (2000) Characterization of YpmQ, an accessory protein required for the expression of cytochrome *c* oxidase in *Bacillus subtilis*. *J. Biol. Chem. 275*, 28802–28809.
10. Nittis, T., George, G. N., and Winge, D. R. (2001) Yeast Sco1, a protein essential for cytochrome *c* oxidase function is a Cu(I)-binding protein. *J. Biol. Chem. 276*, 42520–42526.
11. Andruzzi, L., Nakano, M., Nilges, M. J., and Blackburn, N. J. (2005) Spectroscopic studies of metal binding and metal selectivity in *Bacillus subtilis* BSco, a Homologue of the Yeast Mitochondrial Protein Sco1p. *J. Am. Chem. Soc. 127*, 16548–16558.
12. Abriata, L. A., Banci, L., Bertini, I., Ciofi-Baffoni, S., Gkazonis, P., Spyroulias, G. A., Vila, A. J., and Wang, S. (2008) Mechanism of Cu (A) assembly. *Nat. Chem. Biol. 4*, 599–601.
13. Banci, L., Bertini, I., Calderone, V., Ciofi-Baffoni, S., Mangani, S., Martinelli, M., Palumaa, P., and Wang, S. (2006) A hint for the function of human Sco1 from different structures. *Proc. Natl. Acad. Sci. U.S.A. 103*, 8595–8600.
14. Seib, K. L., Jennings, M. P., and McEwan, A. G. (2003) A Sco homologue plays a role in defence against oxidative stress in pathogenic *Neisseria*. *FEBS Lett. 546*, 411–415.
15. Davidson, D. E., and Hill, B. C. (2009) Stability of oxidized, reduced and copper bound forms of *Bacillus subtilis* Sco. *Biochim. Biophys. Acta 1794*, 275–281.
16. Finney, L. A., and O'Halloran, T. V. (2003) Transition metal speciation in the cell: Insights from the chemistry of metal ion receptors. *Science 300*, 931–936.
17. Imriskova-Sosova, I., Ye, Q., Hill, B. C., and Jia, Z. (2003) Purification, crystallization and preliminary X-ray analysis of a Sco1-like protein from *Bacillus subtilis*, a copper-binding protein involved in the assembly of cytochrome *c* oxidase. *Acta Crystallogr. D59*, 1299–1301.
18. Andrews, D., Mattatall, N. R., Arnold, D., and Hill, B. C. (2005) Expression, purification, and characterization of the CuA-cytochrome *c* domain from subunit II of the *Bacillus subtilis* cytochrome *caa*3 complex in *Escherichia coli*. *Protein Expression Purif. 42*, 227–235.
19. Riener, C. K., Kada, G., and Gruber, H. J. (2002) Quick measurement of protein sulfhydryls with Ellman's reagent and with 4,4′-dithiodipyridine. *Anal. Bioanal. Chem. 373*, 266–276.
20. Imriskova-Sosova, I., Andrews, D., Yam, K., Davidson, D., Yachnin, B., and Hill, B. C. (2005) Characterization of the Redox and Metal Binding Activity of BsSco, a Protein Implicated in the Assembly of Cytochrome *c* Oxidase. *Biochemistry 44*, 16949–16956.
21. DeSa, R. J., and Matheson, I. B. (2004) A practical approach to interpretation of singular value decomposition results. *Methods Enzymol. 384*, 1–8.
22. Chen, Y., and Barkley, M. D. (1998) Toward understanding tryptophan fluorescence in proteins. *Biochemistry 37*, 9976–9982.
23. Lee, J. C., Gray, H. B., and Winkler, J. R. (2008) Copper(II) binding to α-synuclein, the Parkinson's protein. *J. Am. Chem. Soc. 130*, 6898–6899.
24. Carr, H. S., and Winge, D. R. (2003) Assembly of cytochrome *c* oxidase within the mitochondrion. *Acc. Chem. Res. 36*, 309–316.
25. Guex, N., and Peitsch, M. C. (1997) SWISS-MODEL and the Swiss-PdbViewer: An environment for comparative protein modeling. *Electrophoresis 18*, 2714–2723.
26. Banci, L., Bertini, I., Ciofi-Baffoni, S., Hadjiloi, T., Martinelli, M., and Palumaa, P. (2008) Mitochondrial copper(I) transfer from Cox17 to Sco1 is coupled to electron transfer. *Proc. Natl. Acad. Sci. U.S.A. 105*, 6803–6808.